Crystal structure of mullite: A re-examination of the average structure

Ross J. Angel,* Charles T. Prewitt*

Department of Earth and Space Sciences, State University of New York at Stony Brook, Stony Brook, New York 11794, U.S.A.

Abstract

The average structure of a mullite, $Al_2(Al_{2+x}Si_{2-2x})O_{10-x}$, with composition $x = 0.40$, has been determined by refinement of X-ray diffraction data. Because the mullite structure is incommensurate, the average structure contains information about the modulation in the form of apparently positionally disordered atoms. Although some such atom sites may be adequately described by split-atom models in the least-squares refinement procedure, very small displacements cannot be so described. In this study, third- and fourth-order tensors are used to describe two such oxygen sites. In addition to allowing these small displacements to be identified, the results of the refinement also provide further information regarding the occupancies of the two tetrahedral sites by Si and Al.

Introduction

The mineral mullite, $Al_2(Al_{2+2x}Si_{2-2x})O_{10-x}$, has a stability field intermediate in composition between Al_2SiO_5 and alumina, Al_2O_3. In order to accommodate this compositional variation, which is based upon the exchange $O^{2-} + 2Si^{4+} = 2Al^{3+}$, the structure develops an incommensurate modulation in which the occupancies and positions of the tetrahedral cation sites and some oxygen sites vary through the structure in a periodic way. The eventual goal of this investigation into the mullite structure is the rigorous characterization of this modulation. But before this can be done, the average structure needs to be determined to a greater degree of detail than has previously been achieved. It is the purpose of this paper to describe such a structure determination and to show that the structure so determined provides further information about the nature of the incommensurate modulation.

Previous work

Previous to this study there have been three studies made of the average structure of mullite based upon X-ray structure determination (Sadanaga et al., 1962; Burnham 1963, 1964; Durovic, 1969). Durovic and Fejdi (1976) also reported the results of a structure determination of a mullite phase in which the Si was replaced by Ge. All of these studies agree in their basic conclusions regarding the average structure of mullite, which is best described in relation to the sillimanite structure with which it shares many features.

The mullite structure has a c-axis repeat of about 2.9 Å, half that of sillimanite, but otherwise resembles that structure in possessing columns of edge-sharing AlO_6 oc-

tahedra that form chains running parallel to the **c** axis. At height $z = \frac{1}{2}$ in each mullite cell (corresponding to $z = \frac{1}{4}$, $\frac{3}{4}$ in the sillimanite cell), the octahedral columns are cross-linked by tetrahedrally coordinated Si and Al, the tetrahedra forming double chains that also run parallel to the **c** axis (Fig. 1a). The central oxygen site of these chains (Oc) provides the key to understanding the mullite structure.

If it were possible to derive the mullite structure from that of sillimanite (Al_2SiO_5) by operation of the substitution $O^{2-} + 2Si^{4+} \rightarrow 2Al^{3+}$, it is clear that some oxygens must be removed from the structure. The results of the previous studies all show that it is the Oc site from which oxygen is removed. The two adjacent tetrahedral cation sites (T) are now coordinated by only three oxygen atoms and therefore displace to the T* positions (Fig. 1b). The adjacent Oc site is now three-coordinated by tetrahedral cations, and the oxygen is displaced off the symmetry center toward the T* site. This new oxygen site is designated Oc*.

Combined with these displacements is a replacement of tetrahedral Si by Al. Simple considerations show that the resultant site occupancies should be related to the compositional variable x by

$$O \text{ on Oc: } 1 - \frac{3}{2}x \qquad Si \text{ (T plus T*): } \frac{1}{2} - \frac{1}{2}x$$

$$O \text{ on Oc*: } \frac{1}{2}x \qquad Al \text{ (T plus T*): } \frac{1}{2} + \frac{1}{2}x$$

whereas the total number of atoms should be $1 - x/2$ on the T site, and $x/2$ on the T* site. The total oxygen content of Oc + 2Oc* (Oc being on a special equivalent position of multiplicity two, Oc* on one of multiplicity four) is constrained by the composition of the crystal to be $1 - x/2$. If the occupancy of Oc* by oxygen is correlated with
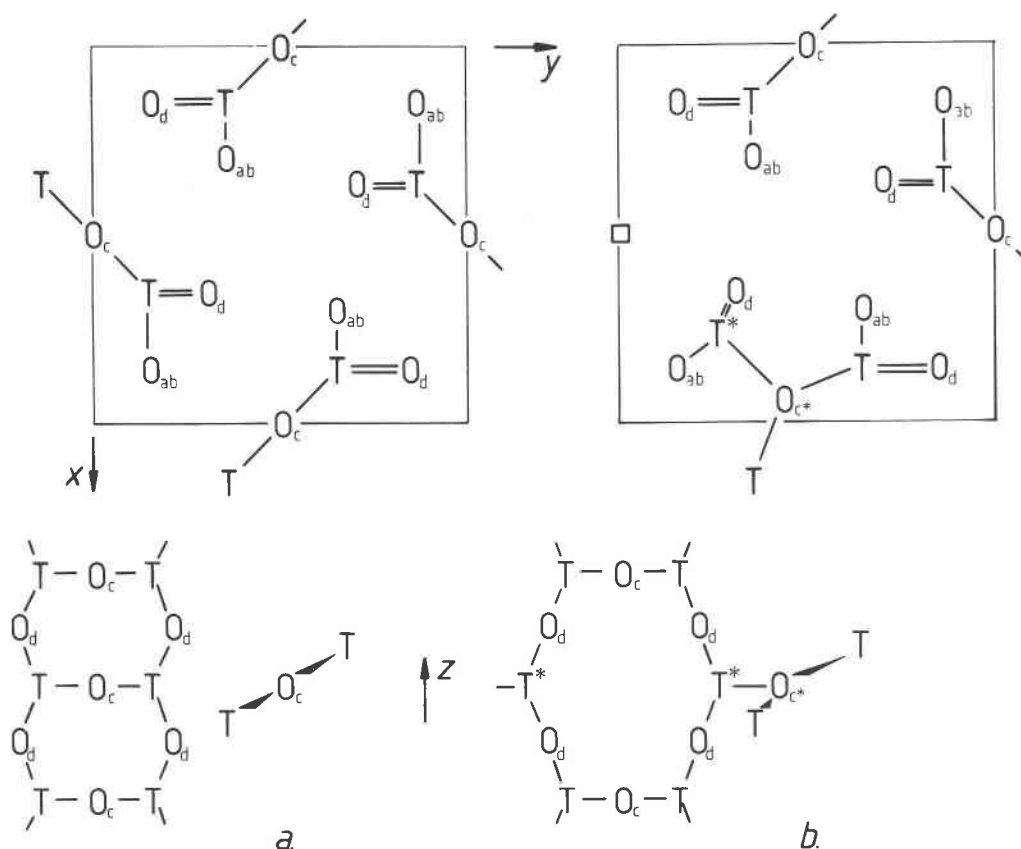
Fig. 1. Idealized representations of the structures of (a) sillimanite and (b) mullite. The octahedrally coordinated Al sites have been omitted for clarity. The upper part of each diagram represents a projection of each structure onto (001); the lower a view of the tetrahedral double chains that run parallel to the c axis. The structure of mullite can be thought of as being derived from that of sillimanite by successive removal of oxygen atoms from the Oc sites and the displacement of adjacent atoms as shown.

occupancy of the T* tetrahedral site, then each Oc* site will be occupied by x oxygen atoms. The occupancy of Oc is then $1 - \frac{3}{2}x$. It should be noted that with this scheme of site occupancies the mullite solid solution will have a high-alumina compositional limit at $x = \frac{2}{3}$, corresponding to a totally vacant Oc site. If the solid solution extends further than this toward the Al_2O_3 composition, oxygen atoms would have to be removed from other positions in the structure.

One outstanding question is the distribution of Al and Si between the T and T* sites in mullite. There is general agreement that the T* site is richer in Al than in Si, but while Sadanaga et al. (1962) considered this site to be exclusively occupied by Al, Burnham (1964) and Durovic and Fejdi (1976) concluded that it is likely that a small proportion of the T* sites are occupied by Si atoms. All of these previous studies also noted that the anisotropic temperature factors of the Oab and Od sites were anomalously large. As these sites coordinate the T and T* tetrahedral sites, these results were interpreted as indicating that the oxygen atoms in these two sites took up slightly different positions dependent upon the occupancy of the adjacent tetrahedral sites. In this study we address the problem of refining these "split" sites by using third- and fourth-order tensors to describe the anharmonic distribution of scattering density associated with the Oab and Od oxygen sites. This has allowed the small displacements of the atoms on these sites to be identified and correlated with possible tetrahedral site occupancies.

EXPERIMENTAL DETAILS

Specimen

The material used for this study was selected from the sample previously described by Cameron (1977) and designated in that paper as "no. 5." It is a commercial fused mullite, this particular sample coming from the center of an ingot, and was therefore

Table 1. Crystallographic data for mullite

a 7.5785(6) Å	Space group: Pbam
b 7.6817(7) Å	
c 2.8864(3) Å	Z = 1
V 168.04(3) Å³	

Note: Estimated standard deviations are in parentheses.

relatively slowly cooled. Cameron (1977) reported the composition as 66.7 mol% Al_2O_3, which corresponds to $x = 0.40$ in the formula $Al_2(Al_{2+2x}Si_{2-2x})O_{10-x}$. A portion of this sample, which is essentially one large single crystal, was crushed, and suitable fragments were mounted for X-ray diffraction. Precession photographs of several fragments showed the systematic absences of Bragg reflections characteristic of *Pbam* symmetry, together with satellites paired around the $l = \frac{1}{2}$ positions. The splitting of these satellites was measured to be $0.30\mathbf{a}^*$, in agreement with Cameron (1977).

Data collection

A Picker four-circle diffractometer with graphite-monochromatized MoKα radiation (λ = 0.7107 Å) was used to collect integrated intensity data of the main reflections up to $2\theta = 110°$ in one octant of reciprocal space. In addition the reflections in a second octant were collected out to $2\theta = 40°$. All reflections were collected with an ω-2θ scan, with a scan width of $2.0° + 0.7°$ tan θ in a constant precision mode. Cell parameters were determined by a constrained least-squares fit to data from 24 reflections in the range $60° < 2\theta < 70°$ that were individually centered at eight equivalent positions on the diffractometer. Cell parameters and other crystallographic data are provided in Table 1.

Refinement

Initial structure refinements and all the Fourier maps were calculated using the Cambridge Crystallography Subroutine Library (CCSL, Matthewman et al., 1982), and the refinement of anharmonic temperature factors was carried out with the REFINE program of the PROMETHEUS program package (Zucker et al., 1983). All refinements were carried out with the data weighted in inverse proportion to the variances of the observations as determined from the parameters of the data collection. Of the 1371 symmetry-allowed reflections collected, 80 were found to have intensities less than twice their estimated standard deviations, and these were excluded from the refinements. None of the remaining 1291 reflections had uneven backgrounds under the criterion of Swanson and Prewitt (1983).

The initial cycles of refinement were carried out using the structural parameters determined by Burnham (1964) as a starting model and using form factors and anomalous dispersion factors for neutral atoms taken from the *International Tables* (1974). However, after convergence of this initial refinement, Fourier maps calculated with coefficients $|F_o| - |F_c|$ and with phases from the refined structure showed significant negative density at positions corresponding to those of the cations within the structure. This prompted a change to form factors for fully charged atoms, the coefficients for the exponential expressions for those of Al^{3+} and Si^{4+} being taken from the *International Tables* (1974) and those for O^{2-} from Hovestreydt (1983).

Refinements with charged-atom form factors showed marginal improvements in R values over those using form factors of neutral atoms. After correction of the data for absorption $[\mu(MoK\alpha) = 10.7 \text{ cm}^{-1}]$ with programs BXLS (Swanson, in prep.) and ABSORB (Finger, unpub.), the refinement converged to $R_u = 4.5$, $R_w = 7.4$, while several intense low-angle reflections showed large negative values of $|F_o| - |F_c|$, indicating the presence of extinction.[1] Correction for secondary extinction was made with the Lorentzian model of Becker and Coppens (1974) using absorption-weighted path lengths to calculate the extinction coefficient, y_s, for each reflection. The two parameters of the extinction model, the domain radius and the mosaic spread, were refined

with the structural parameters to convergence, and the resulting F_c values were used to calculate the parameters y_s, which were in turn applied to correct the F_o values. After this correction was made, the F_o values were averaged over symmetrically equivalent reflections to produce a set of 1143 unique data. Subsequent refinement of the structure converged to $R_u = 3.3$, $R_w = 3.6$.

Because the structure model is used to calculate the extinction correction applied to each reflection, a number of iterations through the extinction correction and averaging of the data are necessary to achieve true convergence. Each iterative cycle consists of using the converged structure from the previous cycle to further refine the parameters of the extinction model and thereby calculate a new set of F_c values; these are in turn used to calculate a set of y_s for application to F_o, which can then be averaged. In this refinement, only one subsequent iteration cycle was found to be necessary, and subsequent refinement of all the structural parameters converged to $R_u = 3.0$, $R_w = 3.5$.

Up to this point in the refinements, the occupancies of the partially occupied sites, Oc, Oc*, T, and T* had been constrained in accordance with the generally accepted model of the average structure (see above). These constraints were now relaxed in several ways in different refinements, the most significant results being achieved by allowing Si into the T* site. In this refinement the total Al and total Si contents of the structure were constrained to be constant, but the distribution of Al and Si between the two tetrahedral sites was allowed to vary. The result was a transfer, relative to the previous model, of Al from the T* site to the T site and an equal transfer of Si in the opposite direction. No constraints were placed on the occupancy of the oxygen sites Oc and Oc*, but it was found that the charge neutrality of the structure was maintained (within one standard deviation) by the refinement without any specific constraint.

Figures 2a and 2b show electron-density maps calculated by Fourier synthesis of the structure factors calculated with this model. The (001) section at $z = 0$ (Fig. 2a) includes only the octahedrally coordinated Al site and the Od site whose oxygen atom is also shared with the tetrahedral sites at $z = -\frac{1}{2}$ and $z = \frac{1}{2}$ (cf. Fig. 1). This Od site, along with the Oab site at $z = \frac{1}{2}$ (Fig. 2b), shows distinct elongation of the electron density parallel to the vector $T \rightarrow T^*$. This was previously noted by Burnham (1964) and is due to small relative displacements between the positions of oxygens coordinating occupied T sites and those coordinating occupied T* sites. In addition, Fourier difference maps using $|F_o| - |F_c|$ as coefficients show extrema of density at three positions (Figs. 2c, 2d), which suggest that the oxygens take up different positions depending on whether the T site is occupied by Al or Si. However, these displacements are sufficiently small to preclude their description as split sites, as correlation between parameters makes the least-squares procedure unstable.

This is in contrast to the third oxygen site, Oc, which was quite adequately described in terms of partial occupancy of the symmetry center at $\frac{1}{2} 0 \frac{1}{2}$, together with a second site, Oc*, at $0.45\ 0.05\ \frac{1}{2}$, although there were also high correlations between the parameters of the two sites. The significance of the refined values of these parameters was therefore tested by carrying out a refinement of the Oc* parameters alone to only those structure factors of reflections with $h + k = $ odd, to which scattering from the Oc atoms does not contribute. No significant change in the parameters of the Oc* site were observed.

In order to describe the distribution of scattering density at the Oab and Od sites, use was made of anharmonic temperature factors to modify the structure-factor equation. The interpretation of these third- and higher-rank tensors is discussed below. The PROMETHEUS program was used to refine the values of allowed coefficients of the third- and fourth-rank tensors for the Oab and

---

[1] The R values are defined as $R_u = \Sigma(|F_o| - |F_c|)/|F_o|$ and $R_w = [\Sigma\ w(|F_o| - |F_c|)^2/\Sigma\ |F_o|^2]^{\frac{1}{2}}$.
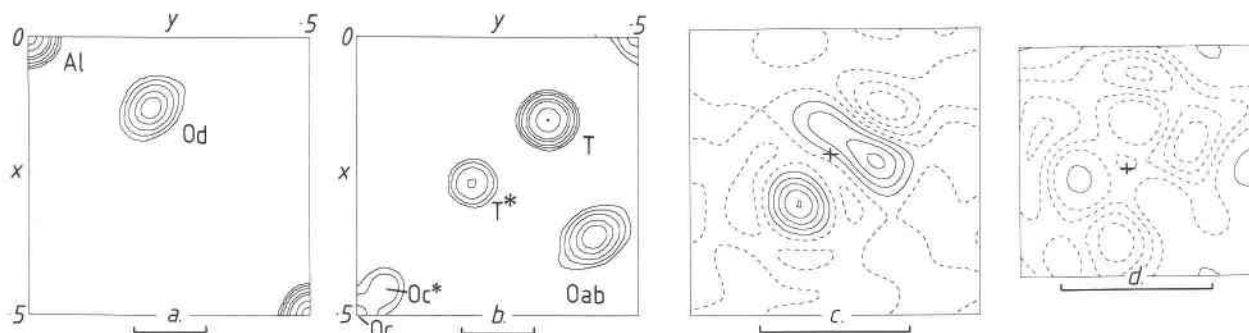
Fig. 2. Fourier maps calculated before the introduction of high-order tensors into the refinement. Sections parallel to (001) of the calculated electron density are shown at (a) $z = 0$ and (b) $z = \frac{1}{2}$. Contours are at 90, 60, 30, 20, 10, 5, and 2.5 electrons/Å³. The limitations of the harmonic model are shown by the Fourier difference functions around the (c) Oab site (section at $z = \frac{1}{2}$) and (d) the Od site (section at $z = 0$). Contours at 0.2 e/Å³ intervals for (c), with the lowest at -0.7 e/Å³, and at 0.1 e/Å³ intervals for (d), with the lowest at -0.4 e/Å³. Negative contours are represented by broken lines, and all scale bars represent 1 Å.

Od atoms in the Gram-Charlier formulation of the structure-factor equation (Johnson and Levy, 1974). In this expansion the harmonic temperature factor of an atom, $\exp(-b_{ij}H_iH_j)$, is multiplied by as many terms of the series:

$$1 + \frac{(i\pi)^3}{3!}c_{ijk}H_iH_jH_k$$
$$+ \frac{(i\pi)^4}{4!}d_{lmno}H_lH_mH_nH_o + \ldots \quad (1)$$

as desired, where c_{ijk} and d_{lmno} are the components of third- and fourth-rank tensors. This particular expansion is preferred over various alternatives because it can be terminated at any arbitrary order without introducing errors into its Fourier transform (Zucker and Schultz, 1982a).

After introduction of the third- and fourth-rank tensors to describe the Oab site, the R values fell to $R_u = 2.6$ and $R_w = 2.9$,

a large and significant improvement. A further but smaller improvement to the final values of $R_u = 2.45$ and $R_w = 2.67$ followed the refinement of the tensor coefficients for the Od site. The structural parameters and temperature factors obtained from this refinement are listed in Table 2. The calculated and observed structure factors are listed in Table 3.[2]

DISCUSSION

The results of this structure determination are in general agreement with those previously reported for the mullite structure (Sadanaga et al., 1962; Burnham, 1964; Durovic, 1969; Durovic and Fejdi, 1976). The differences in struc-

[2] To receive a copy of Table 3, order Document AM-86-321 from the Business Office, Mineralogical Society of America, 1625 I Street, N.W., Suite 414, Washington, D.C. 20006, U.S.A. Please remit $5.00 in advance for the microfiche.

Table 2. Structural parameters for mullite

	Al	T	T*	Oab	Oc	Oc*	Od
x	0.0	0.14901(2)	0.26247(9)	0.3590(1)	0.5	0.4498(4)	0.1273(1)
y	0.0	0.34026(2)	0.20529(9)	0.4218(1)	0.0	0.0505(4)	0.2186(1)
z	0.0	0.5	0.5	0.5	0.5	0.5	0.0
occ.	1.0	0.56(2) Al 0.25(2) Si	0.13(2) Al 0.06(2) Si	1.0	0.39(1)	0.19(1)	1.0
β_{11}	0.00311(2)	0.00255(2)	0.00248(9)	0.0049(1)	0.0061(3)	0.0039(3)	0.0053(1)
β_{22}	0.00266(2)	0.00310(2)	0.00326(9)	0.0063(1)	0.0052(4)	0.0026(3)	0.0045(1)
β_{33}	0.01660(15)	0.02206(16)	0.01628(62)	0.0176(3)	0.0609(18)	0.0386(17)	0.0308(8)
β_{12}	0.00023(2)	$-0.00016(1)$	0.00012(6)	$-0.0024(1)$	$-0.0012(4)$	$-0.0003(2)$	$-0.0022(1)$
B_{eq}	0.63	0.68	0.63	1.06	1.56	0.93	1.10

	Third-order tensor coefficients ($\times 10^5$)				Fourth-order tensor coefficients ($\times 10^6$)	
	Oab	Od			Oab	Od
c_{111}	0.145(13)	$-0.060(13)$		d_{1111}	$-0.025(8)$	$-0.028(9)$
c_{222}	$-0.009(13)$	$-0.033(13)$		d_{2222}	$-0.086(9)$	$-0.042(7)$
c_{112}	$-0.134(8)$	0.027(8)		d_{3333}	$-0.101(371)$	$-1.450(388)$
c_{122}	0.101(8)	0.014(7)		d_{1112}	$-0.001(4)$	$-0.001(1)$
c_{133}	$-0.054(39)$	0.092(49)		d_{1122}	$-0.010(3)$	$-0.006(3)$
c_{233}	0.024(45)	0.363(45)		d_{1133}	0.010(18)	$-0.010(24)$
				d_{1222}	0.033(5)	0.008(4)
				d_{1233}	0.024(14)	0.001(16)
				d_{2233}	$-0.030(19)$	$-0.046(21)$

Note: Estimated standard deviations are given in parentheses.

Table 4a. Interatomic distances and bond angles for the average structure

Distances (Å)			Angles (°)		
			Al site		
Al–Oab	[4]	1.8936(5)	Oab–Al–Oab	[4]	99.31(4)
Al–Od	[2]	1.9366(9)	Oab–Al–Oab	[2]	180.0(−)
			Oab–Al–Od	[8]	90.34(3)
			Od–Al–Od	[1]	180.0(−)
			T site		
T–Oab	[1]	1.7102(8)	Oab–T–Oc	[1]	111.15(3)
T–Oc	[1]	1.6676(2)	Oab–T–Od	[2]	106.66(3)
T–Od	[2]	1.7273(5)	Oc–T–Od	[2]	109.50(3)
Average		1.708(1)	Od–T–Od	[1]	113.34(5)
			T* site		
T*–Oab	[1]	1.8166(11)	Oab–T*–Oc*	[1]	106.21(7)
T*–Oc*	[1]	1.8522(41)	Oab–T*–Od	[2]	100.37(5)
T*–Od	[2]	1.7727(7)	Oc*–T*–Od	[2]	118.68(5)
Average		1.803(5)	Od–T*–Od	[1]	109.01(6)

Note: Multiplicities are indicated by figures in square brackets. Estimated standard deviations are given in parentheses.

Table 4b. Interatomic distances for the tetrahedral sites

	Oxygen position for Al on T	(Å)	Oxygen position for Si on T	(Å)
T–Oab	0.355, 0.462, 0.5	1.81	?	<1.81
–Oc	0.500, 0.000, 0.5	1.67	0.500, 0.000, 0.0	1.67
–Od	0.075, 0.225, 0.0	1.78	0.160, 0.260, 0.0	1.57
Average		1.76		<1.66
T*–Oab	0.405, 0.390, 0.5	1.78		
–Oc*	0.450, 0.051, 0.5	1.85		
–Od	0.135, 0.175, 0.0	1.75		
Average		1.78		

tural parameters between the various refinements may be attributed to compositional differences between samples, whereas all the refinements report temperature factors that appear to be anomalously large when compared with those determined in a study of the Al_2SiO_5 polymorphs (e.g., Winter and Ghose, 1979). The fact that all refinements of mullite have resulted in large values of these parameters suggests that such values are "real" and are related to an attempt by the least-squares procedure to describe an apparently diffuse scattering-density distribution arising from the fact that the mullite structure is incommensurate.

Contrary to the view of Sadanaga et al. (1962), but in agreement with the results of Burnham (1964) and Durovic (1969), the refinement of tetrahedral site occupancies resulted in a small amount of Si being transferred into the T* site. The resultant occupancies (Table 2) suggest that the ratio of Al to Si is the same (2:1) in both of the tetrahedral sites. However, in view of the uncertainties associated with these occupancies, the results are not conclusive, and the problem is unlikely to be resolvable by direct refinement of the occupancies, not only because Al and Si have such similar scattering factors, but also because an extra degree of freedom is introduced into the refinement by the fact that the sites are not fully occupied. Even the results of a refinement of a mullite structure in which the Si had been replaced by Ge (Durovic and Fejdi, 1976) were similarly inconclusive.

Tetrahedral bond distances have often been used as an alternative indicator of the occupancies of such sites (e.g., Kroll and Ribbe, 1983). It is observed that the oxygen atoms move in toward sites enriched in Si and away from those enriched in Al, while there is usually no significant movement of the tetrahedral cation (e.g., Wenk et al., 1980). This is clearly the case in mullite, as the calculated electron-density map (Fig. 2b) shows no evidence of distortion of the two tetrahedral sites. The bond lengths calculated from the structural parameters obtained in this refinement (Table 4a) show that the T site is intermediate

in size between the Si^{iv} and Al^{iv} sites of sillimanite (Winter and Ghose, 1979), which is consistent with the mixed Al-Si content assigned to it by the least-squares procedure. However, the T* site is not only significantly larger than the Al^{iv} site of sillimanite, as would be expected from a site only 20% occupied, but it is also considerably more distorted. This distortion partly arises because the average positions of the oxygen sites are being used for the calculation of bond lengths. In an incommensurate structure these average positions do not necessarily represent the actual positions occupied by atoms in the structure. It is therefore necessary to consider in more detail the information provided by the refinement concerning the Oab and Od sites.

The Oab and Od sites

It should be recalled that the structure obtained by refinement of X-ray-diffraction intensity data represents a time-and-space average over all the atoms in the structure. In ordered crystalline materials this reduces to an average of the small displacements of the atoms from their mean positions (identical in every cell), which are associated with thermal vibrations. In most structures this thermal motion is adequately described by assuming the atoms to be moving in a harmonic potential, which results in the Fourier transform of the time-average of the charge distribution being described by the familiar symmetric second-rank tensor, the anisotropic temperature factor. This assumption of harmonic motion has already been shown to be inappropriate in materials such as fast-ionic conductors (e.g., Zucker and Schultz, 1982b). In these materials the ions responsible for conduction occupy large cavities in which the potential is far from harmonic, and the contribution from the scattering density associated with such ions is clearly misrepresented by the use of a purely harmonic temperature factor in the structure-factor equation. The general solution to this problem has been to describe the departure from harmonicity of the potential by the introduction of higher-order tensors into the structure-factor equation. Consideration of Equation 1 shows that tensors of odd rank make an antisymmetric contribution to the structure factor and thus represent skewness in the potential, whereas tensors of even rank make a symmetric contribution and thus describe the kurtosis of the potential.

The case of fast-ion conductors is quite clearly an example of structures in which some atomic motions show

large deviations from being harmonic. By contrast, in in-commensurate structures, the structure refined from Bragg reflections alone represents not an average of the atoms in the crystal undergoing thermal vibrations about equiv-alent points, but an average of such vibrations about dif-ferent points. To use mullite as an example: An oxygen on an Oab site in a unit cell in which the T site is occupied by Al will vibrate about a different mean position than one in a cell in which the T site is occupied by Si, or one in a third cell where the T* site is occupied instead of the T site. The *average* structure in this case therefore includes the superposition of these three slightly different oxygen sites. Even if each Oab site in each cell could be described in terms of a harmonic potential and thus have a harmonic temperature factor, it is quite obvious that their super-position in the average structure is not harmonic and may be described in terms of higher-rank tensors (Bachmann and Schulz, 1984). It should be noted that although these tensors are often termed "higher-order temperature fac-tors" we are not, in this case, making any judgment about the harmonicity or otherwise of the motion of individual oxygen atoms.

The physical significance of these tensors can best be seen by examining the Fourier maps presented in Figures 3a–3d. These are all (001) sections through the cell at a height $z = \frac{1}{2}$, chosen to pass through the center of the Oab atom position. Figure 3a is the calculated electron density using third- and fourth-rank tensors and is essentially the same as that calculated without the addition of these ten-sors (cf. Fig. 2b). The difference maps calculated after the introduction of each tensor (Figs. 3b, 3c) show how the antisymmetric contribution from the third-rank tensor tends to make the difference map more symmetric, where-as the fourth-rank tensor evens out the radial distribution of the residual density. Because the resultant overall den-sity (Fig. 3a) tends to obscure the local maxima, it is informative to calculate a Fourier map using as coeffi-cients the difference between F calculated with the higher-rank tensor coefficients included and F calculated without them (i.e., a harmonic model). The resultant map (Fig. 3d), which is analogous to the skew maps of Johnson (1969), represents differences from a purely harmonic model of the average structure and thus highlights the different positions taken up by the oxygen atoms in dif-ferent cells within the structure.

This map shows two obvious maxima, the central co-ordinates of which were used to calculate T–Oab and T*–Oab bond distances (Table 4b). The maximum at 0.405,0.390,0.5 represents the position of the oxygen at-oms in unit cells in which the T* site is occupied, and the corresponding T*–Oab bond distance is 1.78 Å, compared to 1.817 Å calculated from the average Oab position and to a maximum Al^{iv}–O bond distance in sillimanite of 1.796 Å. The more intense maximum in the skew map of the Oab site is connected with occupancy of the T site. If its maximum point is used to calculate bond lengths, the T–Oab distance is increased to 1.81 Å from the value of 1.71 Å calculated from the average position. However, the maximum in the skew map is significantly elongated
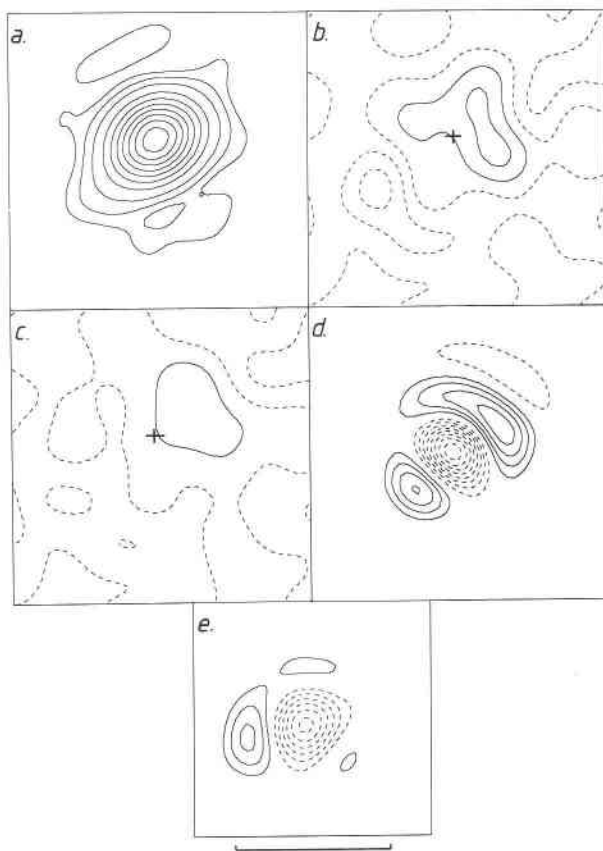

Fig. 3. (a) (001) section at $z = \frac{1}{2}$ of the calculated electron density centered on the Oab site after the introduction of both third- and fourth-order tensors into the refinement. (b) (001) section at $z = \frac{1}{2}$ of the Fourier difference function around the Oab site, after the introduction of the third-order tensor, and (c) after the introduction of the fourth-order tensor. The difference between the final refinement with fourth-order tensors and the harmonic model is shown in (001) sections of the skew map around (d) the Oab site (at $z = \frac{1}{2}$), and (e) around the Od site (at $z = 0$). The scale bar represents 1 Å for all of the maps. The contour levels are as follows (in electrons/Å³): (a) 1.25, 2.5, 5.0, then at intervals of 5. (b and c) Lowest positive contour at 0.1; intervals of 0.2. (d and e) Lowest positive contour at 0.25; in-tervals of 0.2.

toward the T site, suggesting that the oxygen is displaced toward the T site when that site is occupied by Si instead of Al. The longer bond distance of 1.81 Å is therefore an estimate of the Al^T–Oab bond length.

The skew map of the Od site (Fig. 3e) shows three maxima; the one at 0.16,0.26,0.0 corresponds to shorter T–Od and T*–Od bond lengths (1.57 and 1.62 Å) than the average position of the Od site and thus to Si in one or both of the tetrahedral sites. The remaining two max-ima correspond to Al in the T and T* sites with bond lengths of 1.78 and 1.75 Å, respectively.

It should be noted that in this analysis we have only considered displacements of the Oab and Od atoms within the x-y plane. The large values of the tensor coefficient d_{3333} for both of these sites (Table 2) suggests that they

also either undergo displacements parallel to the **c** axis or that the thermal vibrations in this direction have a strong anharmonic component. Without a study of the mullite structure at a number of different temperatures, it is not possible to distinguish between these two possible contributions.

Tetrahedral site occupancies

When the bond lengths are calculated using the oxygen positions derived from the skew maps, the tetrahedral site configurations given in Table 4b are obtained. These new data represent new evidence for the determination of the occupancies of these sites, particularly whether any Si occupies the T* site. Although the results of the least-squares procedure suggest that up to one-fifth of the Si within the structure may reside in the T* site, the evidence from the skew maps of the Oab and Od sites does not support this conclusion. Whereas the skew map of the Od site shows one maximum that could equally well correspond to Si occupancy in either tetrahedral site, the skew map of the Oab site shows an elongated maximum that is interpreted as corresponding to occupation of the T site by Si and Al. By contrast the maximum associated with the T* site being occupied shows no such elongation, suggesting that this tetrahedral site is only occupied by one type of atom. If this T*–Oab bond distance of 1.78 Å and the T*–Oc* bond distance are also considered (1.85 Å), overall the evidence points to very little or no Si residing in the T* site.

CONCLUSIONS

The structure of a member of the mullite solid solution has been determined to a greater resolution than previously achieved. The use of higher-order tensors to describe the averaging of several closely spaced oxygen positions has enabled the small relative displacements of these sites to be correlated with the occupancies of the tetrahedral sites. These displacements suggest that, in agreement with previous work, the occupancy of Si in the T* site is small or zero. However, the refinement of the tetrahedral site occupancies resulted in the same Al/Si ratio in both types of tetrahedral site. Thus we have evidence from the refinement in the form of site occupancies that contradicts evidence obtained from the refined structure in the form of atomic positions and bond lengths.

As the current work probably represents the limit in resolution in determining the Al-Si distribution in mullite by X-ray diffraction, given the similarity in X-ray scattering factors of these two atoms, it is clear that any further progress will require the use of alternative techniques. Possible approaches to the solution of the problem of tetrahedral site occupancies include neutron diffraction or a spectroscopic method such as nuclear magnetic resonance, which is capable of distinguishing Al and Si.

REFERENCES

Bachmann, R., and Schulz, H. (1984) Anharmonic potentials and pseudo potentials in ordered and disordered crystals. Acta Crystallographica, A30, 668–675.

Becker, P.J., and Coppens, P. (1974) Extinction within the limit of validity of the Darwin transfer equations. I. General formalisms for primary and secondary extinction and their application to spherical crystals. Acta Crystallographica, A30, 129–147.

Burnham, C.W. (1963) The crystal structure of mullite. Carnegie Institution of Washington Year Book 62, 158–165.

——— (1964) Crystal structure of mullite. Carnegie Institution of Washington Year Book 63, 223–228.

Cameron, W.E. (1977) Mullite: A substituted alumina. American Mineralogist, 62, 747–755.

Durovic, S. (1969) Refinement of the crystal structure of mullite. Chemicke Zvesti, 23, 113–128.

Durovic, S., and Fejdi, P. (1976) Synthesis and crystal structure of germanium mullite and crystallochemical parameters of D-mullites. Silikaty, 20, 97–112.

Hovestreydt, E. (1983) On the atomic scattering factor for O^{2-}. Acta Crystallographica, A39, 268–269.

International tables for X-ray crystallography. (1974) Kynock Press, Birmingham.

Johnson, C.K. (1969) Addition of higher order cumulants to the crystallographic structure-factor equation: A generalised treatment for thermal motion effects. Acta Crystallographica, A25, 187–194.

Johnson, C.K., and Levy, H.A. (1974) Thermal-motion analysis using Bragg diffraction data. In International tables for X-ray crystallography, volume IV, 311–336. Kynoch Press, Birmingham.

Kroll, H., and Ribbe, P.H. (1983) Lattice parameters, composition and Al/Si order in alkali feldspars. Mineralogical Society of America Reviews in Mineralogy, 2, 57–100.

Matthewman, J.C., Thompson, P., and Brown, P.J. (1982) The Cambridge crystallography subroutine library. Journal of Applied Crystallography, 15, 167–173.

Sadanaga, R., Tokonami, M., and Takéuchi, Y. (1962) The structure of mullite, $2Al_2O_3 \cdot SiO_2$, and relationship with the structures of sillimanite and andalusite. Acta Crystallographica, 15, 65–68.

Swanson, D.K., and Prewitt, C.T. (1983) The crystal structure of $K_2SiSi_3O_9$. American Mineralogist, 68, 581–585.

Wenk, H-R., Joswig, W., Tagai, T., Korekawa, M., and Smith, B.K. (1980) The average structure of An 62–66 labradorite. American Mineralogist, 65, 81–95.

Winter, J.K., and Ghose, S. (1979) Thermal expansion and high temperature crystal chemistry of the Al_2SiO_5 polymorphs. American Mineralogist, 64, 573–586.

Zucker, U.H., and Schultz, H. (1982a) Statistical approaches for the treatment of anharmonic motion in crystals. I. A comparison of the most frequently used formalisms of anharmonic thermal vibrations. Acta Crystallographica, A38, 563–568.

——— (1982b) Statistical approaches for the treatment of anharmonic motion in crystals. II. Anharmonic thermal vibrations and effective atomic potentials in the fast ionic conductor lithium nitride (Li_3N). Acta Crystallographica, A38, 568–576.

Zucker, U.H., Perenthaler, E., Kuhs, W.F., Bachmann, R., and Schultz, H. (1983) PROMETHEUS. A program system for investigation of anharmonic thermal vibrations in crystals. Journal of Applied Crystallography, 16, 358.